Medical Image Analysis (1996) volume 1, number 2, pp 91–108
© Oxford University Press

Deformable models in medical image analysis: a survey

Tim McInerney* and Demetri Terzopoulos

Department of Computer Science, University of Toronto, Toronto, ON, Canada M5S 3H5

Abstract
This article surveys deformable models, a promising and vigorously researched computer-assisted medical image analysis technique. Among model-based techniques, deformable models offer a unique and powerful approach to image analysis that combines geometry, physics and approximation theory. They have proven to be effective in segmenting, matching and tracking anatomic structures by exploiting (bottom-up) constraints derived from the image data together with (top-down) *a priori* knowledge about the location, size and shape of these structures. Deformable models are capable of accommodating the significant variability of biological structures over time and across different individuals. Furthermore, they support highly intuitive interaction mechanisms that, when necessary, allow medical scientists and practitioners to bring their expertise to bear on the model-based image interpretation task. This article reviews the rapidly expanding body of work on the development and application of deformable models to problems of fundamental importance in medical image analysis, including segmentation, shape representation, matching and motion tracking.

Keywords: deformable models, matching, motion tracking, segmentation, shape modeling

Received December 4, 1995; revised March 15, 1996; accepted March 18, 1996

1. INTRODUCTION

The rapid development and proliferation of medical imaging technologies is revolutionizing medicine. Medical imaging allows scientists and physicians to glean potentially life-saving information by peering non-invasively into the human body. The role of medical imaging has expanded beyond the simple visualization and inspection of anatomic structures. It has become a tool for surgical planning and simulation, intra-operative navigation, radiotherapy planning, and for tracking the progress of disease. For example, ascertaining the detailed shape and organization of anatomic structures enables a surgeon preoperatively to plan an optimal approach to some target structure. In radiotherapy, medical imaging allows the delivery of a necrotic dose of radiation to a tumor with minimal collateral damage to healthy tissue.

With medical imaging playing an increasingly prominent role in the diagnosis and treatment of disease, the medical image analysis community has become preoccupied with the challenging problem of extracting—with the assistance of computers—clinically useful information about anatomic structures imaged through CT, MR, PET, and other modalities (Stytz *et al.*, 1991; Robb, 1994; Ayache, 1995a, b; Bizais *et al.*, 1995). Although modern imaging devices provide exceptional views of internal anatomy, the use of computers to quantify and analyze the embedded structures with accuracy and efficiency is limited. Accurate, repeatable, quantitative data must be efficiently extracted in order to support the spectrum of biomedical investigations and clinical activities from diagnosis, to radiotherapy, to surgery.

Segmenting structures from medical images and reconstructing a compact geometric representation of these structures is difficult due to the sheer size of the datasets and the complexity and variability of the anatomic shapes of interest. Furthermore, the shortcomings typical of sampled data, such as sampling artifacts, spatial aliasing and noise, may cause the boundaries of structures to be indistinct and disconnected. The challenge is to extract boundary elements belonging to the same structure and integrate these elements into a coherent and consistent model of the structure. Traditional low-level image-processing techniques which consider only local information can make incorrect assumptions during this integration process and generate infeasible object boundaries.

*Corresponding author
(e-mail: tim@vis.toronto.edu)

As a result, these model-free techniques usually require considerable amounts of expert intervention. Furthermore, the subsequent analysis and interpretation of the segmented objects is hindered by the pixel- or voxel-level structure representations generated by most image-processing operations.

This article surveys deformable models, a promising and vigorously researched model-based approach to computer-assisted medical image analysis. The widely recognized potency of deformable models stems from their ability to segment, match and track images of anatomic structures by exploiting (bottom-up) constraints derived from the image data together with (top-down) *a priori* knowledge about the location, size and shape of these structures. Deformable models are capable of accommodating the often significant variability of biological structures over time and across different individuals. Furthermore, deformable models support highly intuitive interaction mechanisms that allow medical scientists and practitioners to bring their expertise to bear on the model-based image interpretation task when necessary. We will review the basic formulation of deformable models and survey their application to fundamental medical image analysis problems, including segmentation, shape representation, matching and motion tracking.

2. MATHEMATICAL FOUNDATIONS OF DEFORMABLE MODELS

The mathematical foundations of deformable models represent the confluence of geometry, physics and approximation theory. Geometry serves to represent object shape, physics imposes constraints on how the shape may vary over space and time, and optimal approximation theory provides the formal underpinnings of mechanisms for fitting the models to measured data.

Deformable model geometry usually permits broad shape coverage by employing geometric representations that involve many degrees of freedom, such as splines. The model remains manageable, however, because the degrees of freedom are generally not permitted to evolve independently, but are governed by physical principles that bestow intuitively meaningful behavior upon the geometric substrate. The name 'deformable models' stems primarily from the use of elasticity theory at the physical level, generally within a Lagrangian dynamics setting. The physical interpretation views deformable models as elastic bodies which respond naturally to applied forces and constraints. Typically, deformation energy functions defined in terms of the geometric degrees of freedom are associated with the deformable model. The energy grows monotonically as the model deforms away from a specified natural or 'rest shape' and often includes terms that constrain

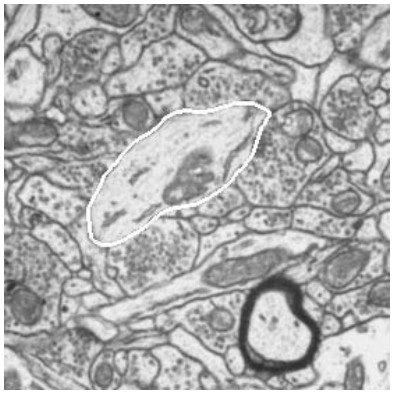


Figure 1. Snake (white) attracted to cell membrane in an EM photomicrograph (Carlbom *et al.*, 1994).

the smoothness or symmetry of the model. In the Lagrangian setting, the deformation energy gives rise to elastic forces internal to the model. Taking a physics-based view of classical optimal approximation, external potential energy functions are defined in terms of the data of interest to which the model is to be fitted. These potential energies give rise to external forces which deform the model such that it fits the data.

Deformable curve, surface and solid models gained popularity after they were proposed for use in computer vision (Terzopoulos *et al.*, 1988) and computer graphics (Terzopoulos and Fleischer, 1988) in the mid-1980s. Terzopoulos introduced the theory of continuous (multidimensional) deformable models in a Lagrangian dynamics setting (Terzopoulos, 1986a), based on deformation energies in the form of (controlled-continuity) generalized splines (Terzopoulos, 1986b). Ancestors of the deformable models now in common use include Fischler and Elshlager's spring-loaded templates (1973) and Widrow's rubber mask technique (1973).

The deformable model that has attracted the most attention to date is popularly known as 'snakes' (Kass *et al.*, 1988). Snakes or 'deformable contour models' represent a special case of the general multidimensional deformable model theory (Terzopoulos, 1986a). We will review their simple formulation in the remainder of this section in order to illustrate with a concrete example the basic mathematical machinery that is present in many deformable models.

Snakes are planar deformable contours that are useful in several image analysis tasks. They are often used to approximate the locations and shapes of object boundaries in images based on the reasonable assumption that boundaries are piecewise continuous or smooth (Figure 1). In its basic form, the mathematical formulation of snakes draws from the theory of optimal approximation involving functionals.

2.1. Energy-minimizing deformable models

Geometrically, a snake is a parametric contour embedded in the image plane $(x, y) \in \Re^2$. The contour is represented as $\boldsymbol{v}(s) = (x(s), y(s))^\top$, where x and y are the coordinate functions and $s \in [0, 1]$ is the parametric domain. The shape of the contour subject to an image $I(x, y)$ is dictated by the functional

$$\mathcal{E}(\boldsymbol{v}) = \mathcal{S}(\boldsymbol{v}) + \mathcal{P}(\boldsymbol{v}). \tag{1}$$

The functional can be viewed as a representation of the energy of the contour and the final shape of the contour corresponds to the minimum of this energy. The first term of the functional,

$$\mathcal{S}(\boldsymbol{v}) = \int_0^1 w_1(s) \left| \frac{\partial \boldsymbol{v}}{\partial s} \right|^2 + w_2(s) \left| \frac{\partial^2 \boldsymbol{v}}{\partial s^2} \right|^2 \mathrm{d}s, \tag{2}$$

is the internal deformation energy. It characterizes the deformation of a stretchy, flexible contour. Two physical parameter functions dictate the simulated physical characteristics of the contour: $w_1(s)$ controls the 'tension' of the contour while $w_2(s)$ controls its 'rigidity'[a]. The second term in (1) couples the snake to the image. Traditionally,

$$\mathcal{P}(\boldsymbol{v}) = \int_0^1 P(\boldsymbol{v}(s))\, \mathrm{d}s, \tag{3}$$

where $P(x, y)$ denotes a scalar potential function defined on the image plane. To apply snakes to images, external potentials are designed whose local minima coincide with intensity extrema, edges and other image features of interest. For example, the contour will be attracted to intensity edges in an image $I(x, y)$ by choosing a potential $P(x, y) = -c|\nabla[G_\sigma * I(x, y)]|$, where c controls the magnitude of the potential, ∇ is the gradient operator, and $G_\sigma * I$ denotes the image convolved with a (Gaussian) smoothing filter whose characteristic width σ controls the spatial extent of the local minima of P.

In accordance with the calculus of variations, the contour $\boldsymbol{v}(s)$ which minimizes the energy $\mathcal{E}(\boldsymbol{v})$ must satisfy the Euler–Lagrange equation

$$-\frac{\partial}{\partial s}\left(w_1 \frac{\partial \boldsymbol{v}}{\partial s}\right) + \frac{\partial^2}{\partial s^2}\left(w_2 \frac{\partial^2 \boldsymbol{v}}{\partial s^2}\right) + \nabla P(\boldsymbol{v}(s, t)) = \boldsymbol{0}. \tag{4}$$

This vector-valued partial differential equation expresses the balance of internal and external forces when the contour rests at equilibrium. The first two terms represent the internal stretching and bending forces respectively, while the third term represents the external forces that couple the snake to the image data. The usual approach to solving (4) is through the application of numerical algorithms (section 2.3).

[a]The values of the non-negative functions $w_1(s)$ and $w_2(s)$ determine the extent to which the snake can stretch or bend at any point s on the snake. For example, increasing the magnitude of $w_1(s)$ increases the 'tension' and tends to eliminate extraneous loops and ripples by reducing the length of the snake. Increasing $w_2(s)$ increases the bending 'rigidity' of the snake and tends to make the snake smoother and less flexible. Setting the value of one or both of these functions to zero at a point s permits discontinuities in the contour at s.

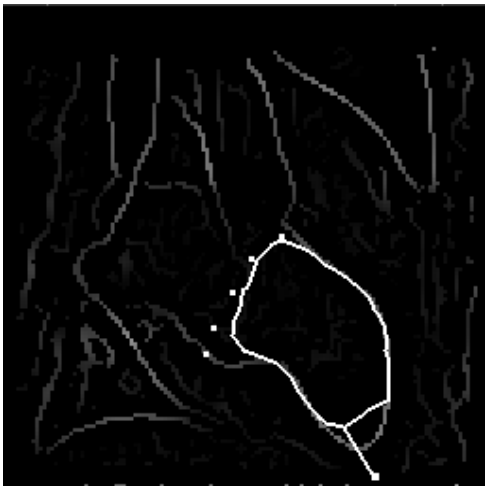


Figure 2. Snake deforming towards high gradients in a processed cardiac image, influenced by 'pin' points and an interactive 'spring' which pulls the contour towards an edge (McInerney and Terzopoulos, 1995a).

2.2. Dynamic deformable models

While it is natural to view energy minimization as a static problem, a potent approach to computing the local minima of a functional such as (1) is to construct a dynamical system that is governed by the functional and allow the system to evolve to equilibrium. The system may be constructed by applying the principles of Lagrangian mechanics. This leads to dynamic deformable models that unify the description of shape and motion, making it possible to quantify not just static shape, but also shape evolution through time. Dynamic models are valuable for medical image analysis, since most anatomical structures are deformable and continually undergo non-rigid motion *in vivo*. Moreover, dynamic models exhibit intuitively meaningful physical behaviors, making their evolution amenable to interactive guidance from a user (Figure 2).

A simple example is a dynamic snake which can be represented by introducing a time-varying contour $\boldsymbol{v}(s, t) = (x(s, t), y(s, t))^\top$ with a mass density $\mu(s)$ and a damping density $\gamma(s)$. The Lagrange equations of motion for a snake with the internal energy given by (2) and external energy given by (3) is

$$\mu \frac{\partial^2 \boldsymbol{v}}{\partial t^2} + \gamma \frac{\partial \boldsymbol{v}}{\partial t} - \frac{\partial}{\partial s}\left(w_1 \frac{\partial \boldsymbol{v}}{\partial s}\right) + \frac{\partial^2}{\partial s^2}\left(w_2 \frac{\partial^2 \boldsymbol{v}}{\partial s^2}\right) = -\nabla P(\boldsymbol{v}(s, t)). \tag{5}$$

The first two terms on the left-hand side of this partial differential equation represent inertial and damping forces. Referring to (4), the remaining terms represent the internal stretching and bending forces, while the right-hand side represents the external forces. Equilibrium is achieved when the internal and external forces balance and the contour comes to rest (i.e. $\partial \boldsymbol{v}/\partial t = \partial^2 \boldsymbol{v}/\partial t^2 = 0$), which yields the equilibrium condition (4).

2.3. Discretization and numerical simulation

In order to compute a minimum energy solution numerically, it is necessary to discretize the energy $\mathcal{E}(\boldsymbol{v})$. The usual approach is to represent the continuous geometric model $\boldsymbol{v}$ in terms of linear combinations of local-support or global-support basis functions. Finite elements (Zienkiewicz and Taylor, 1989), finite differences (Press *et al.*, 1992) and geometric splines (Farin, 1993) are local representation methods, whereas Fourier bases (Ballard and Brown, 1982) are global representation methods. The continuous model $\boldsymbol{v}(s)$ is represented in discrete form by a vector $\boldsymbol{u}$ of shape parameters associated with the basis functions. The discrete form of energies such as $\mathcal{E}(\boldsymbol{v})$ for the snake may be written as

$$E(\boldsymbol{u}) = \tfrac{1}{2}\boldsymbol{u}^\top \mathsf{K}\boldsymbol{u} + \mathrm{P}(\boldsymbol{u}) \tag{6}$$

where K is called the *stiffness matrix*, and $\mathrm{P}(\boldsymbol{u})$ is the discrete version of the external potential. The minimum energy solution results from setting the gradient of (6) to $\boldsymbol{0}$, which is equivalent to solving the set of algebraic equations

$$\mathsf{K}\boldsymbol{u} = -\nabla \mathrm{P} = \boldsymbol{f} \tag{7}$$

where $\boldsymbol{f}$ is the generalized external force vector.

The discretized version of the Lagrangian dynamics equation (5) may be written as a set of second-order ordinary differential equations for $\boldsymbol{u}(t)$:

$$\mathsf{M}\ddot{\boldsymbol{u}} + \mathsf{C}\dot{\boldsymbol{u}} + \mathsf{K}\boldsymbol{u} = \boldsymbol{f}, \tag{8}$$

where M is the mass matrix and C is a damping matrix. The time derivatives in (5) are approximated by finite differences and explicit or implicit numerical time-integration methods are applied to simulate the resulting system of ordinary differential equations in the shape parameters $\boldsymbol{u}$.

2.4. Probabilistic deformable models

An alternative view of deformable models emerges from casting the model fitting process in a probabilistic framework. This permits the incorporation of prior model and sensor model characteristics in terms of probability distributions. The probabilistic framework also provides a measure of the uncertainty of the estimated shape parameters after the model is fitted to the image data (Szeliski, 1990).

Let $\boldsymbol{u}$ represent the deformable model shape parameters with a prior probability $p(\boldsymbol{u})$ on the parameters. Let $p(I|\boldsymbol{u})$ be the imaging (sensor) model—the probability of producing an image I given a model $\boldsymbol{u}$. Bayes' theorem

$$p(\boldsymbol{u}|I) = \frac{p(I|\boldsymbol{u})p(\boldsymbol{u})}{p(I)} \tag{9}$$

expresses the posterior probability $p(\boldsymbol{u}|I)$ of a model given the image, in terms of the imaging model and the prior probabilities of model and image.

It is easy to convert the internal energy measure (2) of the deformable model into a prior distribution over expected shapes, with lower energy shapes being the more likely. This is achieved using a Boltzmann (or Gibbs) distribution of the form

$$p(\boldsymbol{u}) = \frac{1}{Z_s}\exp(-S(\boldsymbol{u})), \tag{10}$$

where $S(\boldsymbol{u})$ is the discretized version of $\mathcal{S}(\boldsymbol{v})$ in (2) and Z_s is a normalizing constant (called the partition function). This prior model is then combined with a simple sensor model based on linear measurements with Gaussian noise

$$p(I|\boldsymbol{u}) = \frac{1}{Z_I}\exp(-\mathrm{P}(\boldsymbol{u})), \tag{11}$$

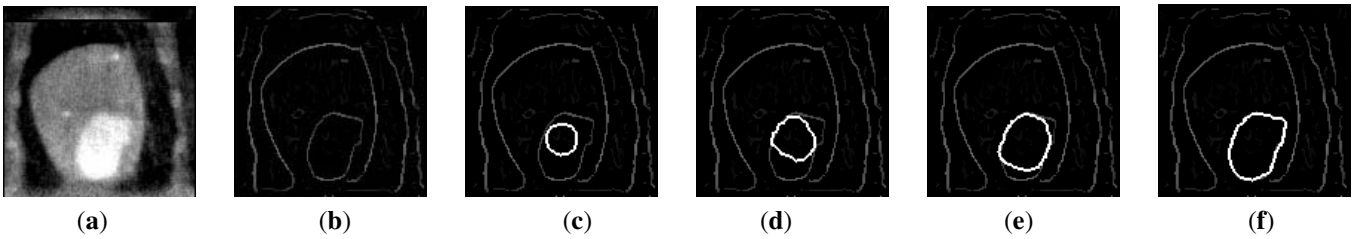
where $\mathrm{P}(\boldsymbol{u})$ is a discrete version of the potential $\mathcal{P}(\boldsymbol{v})$ in (3), which is a function of the image $I(x, y)$.

Models may be fitted by finding $\boldsymbol{u}$ which locally maximize $p(\boldsymbol{u}|I)$ in (9). This is known as the maximum *a posteriori* solution. With the above construction, it yields the same result as minimizing (1), the energy configuration of the deformable model given the image.

The probabilistic framework can be extended by assuming a time-varying prior model, or system model, in conjunction with the sensor model, resulting in a Kalman filter. The system model describes the expected evolution of the shape parameters $\boldsymbol{u}$ over time. If the equations of motion of the physical snakes model (8) are employed as the system model, the result is a sequential estimation algorithm known as 'Kalman snakes' (Terzopoulos and Szeliski, 1992).

3. MEDICAL IMAGE ANALYSIS WITH DEFORMABLE MODELS

Although originally developed for application to problems in computer vision and computer graphics, the potential of deformable models for use in medical image analysis has been quickly realized. They have been applied to images generated by imaging modalities as varied as X-ray, CT, angiography, MR and ultrasound. Two-dimensional and three-dimensional deformable models have been used to segment, visualize,



(**a**) (**b**) (**c**) (**d**) (**e**) (**f**)

Figure 3. (**a**) Intensity CT image slice of LV. (**b**) Edge detected image. (**c**) Initial snake. (**d**)–(**f**) Snake deforming towards LV boundary, driven by 'inflation' force. (McInerney and Terzopoulos, 1995a).

track and quantify a variety of anatomic structures ranging in scale from the macroscopic to the microscopic. These include the brain, heart, face, cerebral, coronary and retinal arteries, kidney, lungs, stomach, liver, skull, vertebra, objects such as brain tumors, a fetus, and even cellular structures such as neurons and chromosomes. Deformable models have been used to track the non-rigid motion of the heart, the growing tip of a neurite and the motion of erythrocytes. They have been used to locate structures in the brain, and to register images of the retina, vertebra and neuronal tissue.

In the following sections, we review and discuss the application of deformable models to medical image interpretation tasks including segmentation, matching and motion analysis.

3.1. Image segmentation with deformable curves

The segmentation of anatomic structures—the partitioning of the original set of image points into subsets corresponding to the structures—is an essential first stage of most medical image analysis tasks, such as registration, labeling and motion tracking. These tasks require anatomic structures in the original image to be reduced to a compact, analytic representation of their shapes. Performing this segmentation manually is extremely labor-intensive and time-consuming. A primary example is the segmentation of the heart, especially the left ventricle (LV), from cardiac imagery. Segmentation of the left ventricle is a prerequisite for computing diagnostic information such as ejection-fraction ratio, ventricular volume ratio, heart output, and for wall motion analysis which provides information on wall thickening etc. (Singh *et al.*, 1993).

Most clinical segmentation is currently performed using manual slice editing. In this scenario, a skilled operator, using a computer mouse or trackball, manually traces the region of interest on each slice of an image volume. Manual slice editing suffers from several drawbacks. These include the difficulty in achieving reproducible results, operator bias, forcing the operator to view each 2-D slice separately to deduce and measure the shape and volume of 3-D structures, and operator fatigue.

Segmentation using traditional low-level image-processing techniques, such as region growing, edge detection and mathematical morphology operations, also requires considerable amounts of expert interactive guidance. Furthermore, automating these model-free approaches is difficult because of the shape complexity and variability within and across individuals. In general, the underconstrained nature of the segmentation problem limits the efficacy of approaches that consider local information only. Noise and other image artifacts can cause incorrect regions or boundary discontinuities in objects recovered by these methods.

A deformable-model-based segmentation scheme, used in concert with image preprocessing, can overcome many of the limitations of manual slice editing and traditional image-processing techniques. These connected and continuous geometric models consider an object boundary as a whole and can make use of *a priori* knowledge of object shape to constrain the segmentation problem. The inherent continuity and smoothness of the models can compensate for noise, gaps and other irregularities in object boundaries. Furthermore, the parametric representations of the models provide a compact, analytical description of object shape. These properties lead to a robust and elegant technique for linking sparse or noisy local image features into a coherent and consistent model of the object.

Among the first and primary uses of deformable models in medical image analysis was the application of deformable contour models, such as snakes (Kass *et al.*, 1988), to segment structures in 2-D images (Berger, 1990; Cohen, 1991; Ueda and Mase, 1992; Rougon and Prêteux, 1993; Cohen and Cohen, 1993; Leitner and Cinquin, 1993; Carlbom *et al.*, 1994; Gupta *et al.*, 1994; Lobregt and Viergever, 1995; Davatzikos and Prince, 1995). Typically users initialized a deformable model near the object of interest (Figure 3) and allowed it to deform into place. Users could then use the interactive capabilities of these models and manually fine-tune them. Furthermore, once the user is satisfied with the result on an initial image slice, the fitted contour model may then be used as the initial boundary approximation for neighboring slices. These models are then deformed into place and again propagated until all slices have been processed. The resulting sequence of 2-D contours can then be connected to form a continuous 3-D surface model (Lin and Chen, 1989; Chang *et al.*, 1991; Cohen, 1991; Cohen and Cohen, 1993).

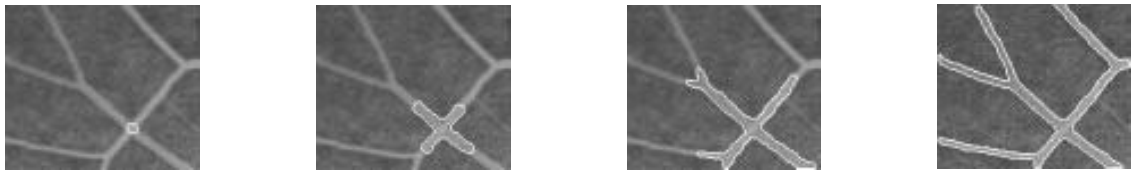
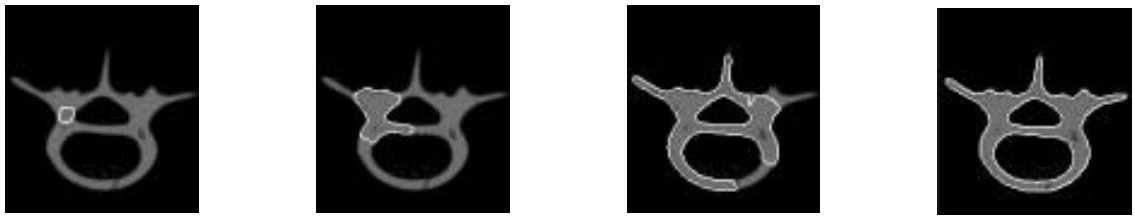


Figure 4. Image sequence of a clipped angiogram of a retina showing an automatically subdividing snake flowing and branching along a vessel (McInerney and Terzopoulos, 1995b).



(**a**) (**b**) (**c**) (**d**)

Figure 5. Segmentation of a cross sectional image of a human vertebra phantom with a topologically adaptable snake (McInerney and Terzopoulos, 1995b). The snake begins as a single closed curve and becomes three closed curves.

The application of snakes and other similar deformable contour models to extract regions of interest is, however, not without limitations. For example, snakes were designed as interactive models. In non-interactive applications, they must be initialized close to the structure of interest to guarantee good performance. The internal energy constraints of snakes can limit their geometric flexibility and prevent a snake from representing long tube-like shapes or shapes with significant protrusions or bifurcations. Furthermore, the topology of the structure of interest must be known in advance since classical deformable contour models are parametric and are incapable of topological transformations without additional machinery.

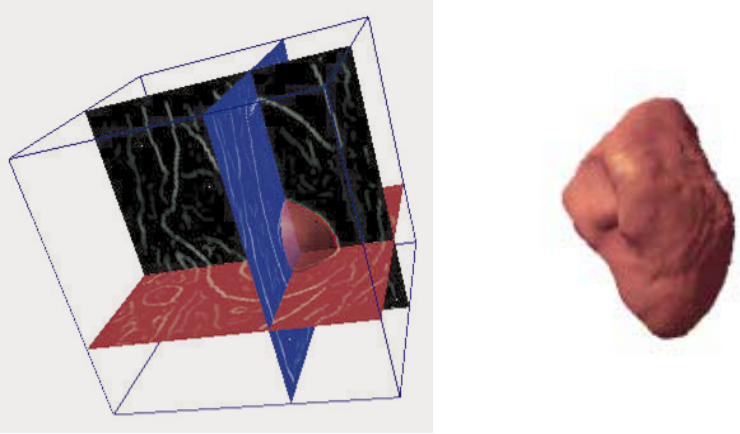
Various methods have been proposed to improve and further automate the deformable contour segmentation process. Cohen and Cohen (1993) used an internal 'inflation' force to expand a snakes model past spurious edges towards the real edges of the structure, making the snake less sensitive to initial conditions [inflation forces were also employed in Terzopoulos *et al.* (1988)]. Amini *et al.* (1990) used dynamic programming to carry out a more extensive search for global minima. Poon *et al.* (1994) and Grzeszczuk and Levin (1994) minimized the energy of active contour models using simulated annealing which is known to give global solutions and allows the incorporation of non-differentiable constraints.

Poon *et al.* (1994) also used a discriminant function to incorporate region-based image features into the image forces of their active contour model. The discriminant function allows the inclusion of additional image features in the segmentation and serves as a constraint for global segmentation consistency (i.e. every image pixel contributes to the discriminant function). The result is a more robust energy functional and a much better tolerance to deviation of the initial guess from the true boundaries. Others researchers (Rougon and Prêteux, 1991; Herlin *et al.*, 1992; Chakraborty *et al.*, 1994; Gauch *et al.*, 1994; Chakraborty and Duncan, 1995; Mangin *et al.*, 1995) have also integrated region-based information into deformable contour models in an attempt to decrease sensitivity to insignificant edges and initial model placement.

Recently, several researchers (Leitner and Cinquin, 1991; Caselles, *et al.*, 1993, 1995; Whitaker, 1994; Malladi *et al.*, 1995; Mc Inerney and Terzopoulos, 1995b; Sapiro *et al.*, 1995) have been developing topology-independent shape modeling schemes that allow a deformable contour or surface model not only to represent long tube-like shapes or shapes with bifurcations (Figure 4), but also dynamically to sense and change its topology (Figure 5).

3.2. Volume image segmentation with deformable surfaces

Segmenting 3-D image volumes slice by slice, either manually or by applying 2-D contour models, is a laborious process and requires a post-processing step to connect the sequence of 2-D contours into a continuous surface. Furthermore, the resulting surface reconstruction can contain inconsistencies or show rings or bands. The use of a true 3-D deformable surface model, on the other hand, can result in a faster, more robust segmentation technique which ensures a globally smooth and coherent surface between image slices. Deformable surface models in 3-D were first used in computer vision (Terzopoulos *et al.*, 1988). Many researchers have since explored the use of deformable surface models for segmenting structures in



(**a**) (**b**)

Figure 6. (**a**) Deformable 'balloon' model embedded in volume image deforming towards LV edges. (**b**) Reconstruction of LV (McInerney and Terzopoulos, 1995a).

medical image volumes. Miller (1991) constructed a polygonal approximation to a sphere and geometrically deformed this 'balloon' model until the balloon surface conforms to the object surface in 3-D CT data. The segmentation process is formulated as the minimization of a cost function where the desired behavior of the balloon model is determined by a local cost function associated with each model vertex. The cost function is a weighted sum of three terms: a deformation potential that 'expands' the model vertices towards the object boundary, an image term that identifies features such as edges and opposes the balloon expansion, and a term that maintains the topology of the model by constraining each vertex to remain close to the centroid of its neighbors.

Cohen and Cohen (1992b; 1993) and McInerney and Terzopoulos (1995a) used finite-element and physics-based techniques to implement an elastically deformable cylinder and sphere, respectively. The models are used to segment the inner wall of the LV of the heart from MR or CT image volumes (Figure 6). These deformable surfaces are based on a thin-plate under tension surface spline, the higher dimensional generalization of Equation (2), which controls and constrains the stretching and bending of the surface. The models are fitted to data dynamically by integrating Lagrangian equations of motion through time in order to adjust the deformational degrees of freedom. Furthermore, the finite-element method is used to represent the models as a continuous surface in the form of weighted sums of local polynomial basis functions. Unlike Miller's (1991) polygonal model, the finite element method provides an analytic surface representation and the use of high-order polynomials means that fewer elements are required to represent an object accurately. Pentland and Sclaroff (1991) and Nastar and Ayache (1993a) also developed physics-based

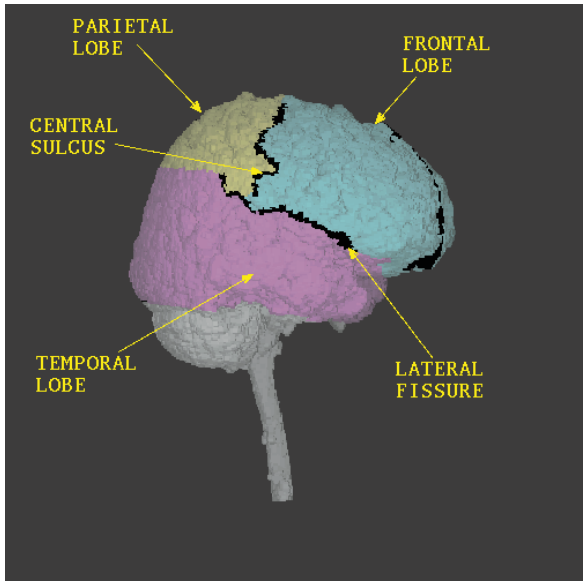


Figure 7. The result of matching a labeled deformable atlas to a morphologically preprocessed MR image of the brain (Sandor and Leahy, 1995).

models but used a reduced modal basis for the finite elements (see section 3.5).

Staib and Duncan (1992b) described a 3-D surface model used for geometric surface matching to 3-D medical image data. The model uses a Fourier parameterization which decomposes the surface into a weighted sum of sinusoidal basis functions. Several different surface types are developed such as tori, open surfaces, closed surfaces and tubes. Surface finding is formulated as an optimization problem using gradient ascent which attracts the surface to strong image gradients

in the vicinity of the model. An advantage of the Fourier parameterization is that it allows a wide variety of smooth surfaces to be described with a small number of parameters. That is, a Fourier representation expresses a function in terms of an orthonormal basis and higher indexed basis functions in the sum represent higher spatial variation. Therefore, the series can be truncated and still represent relatively smooth objects accurately.

In a different approach, Szeliski *et al.* (1993) used a dynamic, self-organizing oriented particle system to model surfaces of objects. The oriented particles, which can be visualized as small, flat disks, evolve according to Newtonian mechanics and interact through external and interparticle forces. The external forces attract the particles to the data while interparticle forces attempt to group the particles into a coherent surface. The particles can reconstruct objects with complex shapes and topologies by 'flowing' over the data, extracting and conforming to meaningful surfaces. A triangulation is then performed which connects the particles into a continuous global model that is consistent with the inferred object surface.

Other notable work involving 3-D deformable surface models and medical image applications can be found in Delingette *et al*. (1992), Whitaker (1994), Tek and Kimia (1995), Davatzikos and Bryan (1995) as well as several models described in the following sections.

3.3. Incorporating *a priori* knowledge

In medical images, the general shape, location and orientation of objects is known and this knowledge may be incorporated into the deformable model in the form of initial conditions, data constraints, constraints on the model shape parameters, or into the model fitting procedure. The use of implicit or explicit anatomical knowledge to guide shape recovery is especially important for robust automatic interpretation of medical images. For automatic interpretation, it is essential to have a model that not only describes the size, shape, location and orientation of the target object but that also permits expected variations in these characteristics. Automatic interpretation of medical images can relieve clinicians from the labor-intensive aspects of their work while increasing the accuracy, consistency and reproducibility of the interpretations.

A number of researchers have incorporated knowledge of object shape into deformable models by using deformable shape templates. These models usually use 'hand-crafted' global shape parameters to embody *a priori* knowledge of expected shape and shape variation of the structures and have been used successfully for many applications of automatic image interpretation. The idea of deformable templates can be traced back to the early work on spring-loaded templates by Fischler and Elshlager (1973). An excellent example in computer vision is the work of Yuille *et al.* (1992) who constructed deformable templates for detecting and describing features of faces, such as the eye. In medical image analysis, Lipson *et al.* (1990) noted that axial cross sectional images of the spine yield approximately elliptical vertebral contours and consequently extracted the contours using a deformable ellipsoidal template.

Deformable models based on superquadrics are another example of deformable shape templates that are gaining in popularity in medical image research. Superquadrics contain a small number of intuitive global shape parameters that can be tailored to the average shape of a target anatomic structure. Furthermore, the global parameters can often be coupled with local shape parameters such as splines resulting in a powerful shape representation scheme. For example, Metaxas and Terzopoulos (1993) employed a dynamic deformable superquadric model (Terzopoulos and Metaxas, 1991) to reconstruct and track human limbs from 3-D biokinetic data. Their models can deform both locally and globally by incorporating the global shape parameters of a superellipsoid with the local degrees of freedom of a membrane spline in a Lagrangian dynamics formulation. The global parameters efficiently capture the gross shape features of the data, while the local deformation parameters reconstruct the fine details of complex shapes. Using Kalman filtering theory, they developed and demonstrated a biokinetic motion tracker based on their deformable superquadric model.

Vemuri and Radisavljevic (1993, 1994) constructed a deformable superquadric model in an orthonormal wavelet basis. This multiresolution basis provides the model with the ability to transform continuously from local to global shape deformations thereby allowing a continuum of shape models to be created and to be represented with relatively few parameters. They applied the model to segment and reconstruct anatomical structures in the human brain from MRI data.

As a final example, Bardinet *et al.* (1995, 1996a, b) fitted a deformable superquadric to segmented 3-D cardiac images and then refined the superquadric fit using a volumetric deformation technique known as free form deformations (FFDs). FFDs are defined by tensor product trivariate splines and can be visualized as a rubber-like box in which the object to be deformed (in this case the superquadric) is embedded. Deformations of the box are automatically transmitted to embedded objects. This volumetric aspect of FFDs allows two superquadric surface models to be simultaneously deformed in order to reconstruct the inner and outer surfaces of the LV of the heart and the volume in between these surfaces. Further examples of deformable superquadrics can be found in Pentland and Horowitz (1991) and Chen *et al.* (1994) (see section 3.5).

Several researchers cast the deformable model fitting process in a probabilistic framework (see section 2.4) and

include prior knowledge of object shape by incorporating prior probability distributions on the shape variables to be estimated (Staib and Duncan, 1992a; Worring *et al.*, 1993; Vemuri and Radisavljevic, 1994). For example, Staib and Duncan (1992a) used a deformable contour model on 2-D echocardiograms and MR images to extract the LV of the heart and the corpus callosum of the brain, respectively. This closed contour model is parameterized using an elliptic Fourier decomposition and *a priori* shape information is included as a spatial probability expressed through the likelihood of each model parameter. The model parameter probability distributions are derived from a set of example object boundaries and serve to bias the contour model towards expected or more likely shapes.

Szekely *et al.* (1996) have also developed Fourier parameterized models. Furthermore, they have added elasticity to their models to create 'Fourier snakes' in 2-D and elastically deformable Fourier surface models in 3-D. By using the Fourier parameterization followed by a statistical analysis of a training set, they define mean organ models and their eigen-deformations. An elastic fit of the mean model in the subspace of eigenmodes restricts possible deformations and finds an optimal match between the model surface and boundary candidates.

Cootes *et al.* (1994) and Hill *et al.* (1993) presented a statistically based technique for building deformable shape templates and use these models to segment various organs from 2-D and 3-D medical images. The statistical parameterization provides global shape constraints and allows the model to deform only in ways implied by the training set. The shape models represent objects by sets of landmark points which are placed in the same way on an object boundary in each input image. For example, to extract the LV from echocardiograms, they chose points around the ventricle boundary, the nearby edge of the right ventricle, and the top of the left atrium. The points can be connected to form a deformable contour. By examining the statistics of training sets of hand-labeled medical images, and using principal component analysis, a shape model is derived that describes the average positions and the major modes of variation of the object points. New shapes are generated using the mean shape and a weighted sum of the major modes of variation. Object boundaries are then segmented using this 'point distribution model' by examining a region around each model point to calculate the displacement required to move it towards the boundary. These displacements are then used to update the shape parameter weights.

3.4. Matching

Matching of regions in images can be performed between the representation of a region and a model (labeling) or between the representation of two distinct regions (registration). Registration of 2-D and 3-D medical images is necessary in order to study the evolution of a pathology in an individual, or to take full advantage of the complementary information coming from multimodality imagery. Recent examples of the use of deformable models to perform medical image registration are found in Bookstein (1989), Moshfeghi (1991), Moshfeghi *et al.* (1994), Gueziec and Ayache (1994), Feldmar and Ayache (1994), Thirion (1994), Hamadeh *et al.* (1995), Lavallée and Szeliski (1995). These techniques primarily consist in constructing highly structured descriptions for matching. This operation is usually carried out by extracting regions of interest with an edge-detection algorithm, followed by the extraction of landmark points or characteristic contours (or curves on extracted boundary surfaces in the case of 3-D data). In 3-D, these curves usually describe differential structures such as ridges, or topological singularities. An elastic matching algorithm can then be applied between corresponding pairs of curves or contours where the 'start' contour is iteratively deformed to the 'goal' contour using forces derived from local pattern matches with the goal contour (Moshfeghi, 1991).

An example of matching where the use of explicit *a priori* knowledge has been embedded into deformable models is the extraction and labeling of anatomic structures in the brain, primarily from MR images. The anatomical knowledge is made explicit in the form of a 3-D brain atlas. The atlas is modeled as a physical object and is given elastic properties. After an initial global alignment, the atlas deforms and matches itself onto corresponding regions in the brain image volume in response to forces derived from image features. The assumption underlying this approach is that at some representational level, normal brains have the same topological structure and differ only in shape details. The idea of modeling the atlas as an elastic object was originated by Broit (1981), who formulated the matching process as a minimization of a cost function. Subsequently, Bajcsy and Kovacic (1989) implemented a multiresolution version of Broit's system where the deformation of the atlas proceeds step-by-step in a coarse-to-fine strategy, increasing the local similarity and global coherence. The elastically deformable atlas technique has since become a very active area of research and is being explored by several researchers (Evans *et al.*, 1991; Bookstein, 1991; Bozma and Duncan, 1992; Gee *et al.*, 1993; Delibasis and Undrill, 1994; McDonald *et al.*, 1994; Christensen *et al.*, 1995; Declerck *et al.*, 1995; Sandor and Leahy, 1995; Snell *et al.*, 1995; Subsol *et al.*, 1995; Davatzikos *et al.*, 1996).

There are several problems with the deformable atlas approach. The technique is sensitive to initial positioning of the atlas—if the initial rigid alignment is off by too much, then the elastic match may perform poorly. The presence of neighboring features may also cause matching problems—the

atlas may warp to an incorrect boundary. Finally, without user interaction, the atlas can have difficulty converging to complicated object boundaries. One solution to these problems is to used image preprocessing in conjunction with the deformable atlas. Sandor and Leahy (1995) used this approach automatically to label regions of the cortical surface that appear in 3-D MR images of human brains (Figure 7). They automatically matched a labeled deformable atlas model to preprocessed brain images, where preprocessing consists of 3-D edge detection and morphological operations. These filtering operations automatically extract the brain and sulci (deep grooves in the cortical surface) from an MR image and provide a smoothed representation of the brain surface to which their 3-D B-spline deformable surface model can rapidly converge.

3.5. Motion tracking and analysis

The idea of tracking objects in time-varying images using deformable models was originally proposed in the context of computer vision (Kass *et al.*, 1988; Terzopoulos *et al.*, 1988). Deformable models have been used to track non-rigid microscopic and macroscopic structures in motion, such as blood cells (Leymarie and Levine, 1993) and neurite growth cones (Gwydir *et al.*, 1994) in cine-microscopy, as well as coronary arteries in cine-angiography (Lengyel *et al.*, 1995). However, the primary use of deformable models for tracking in medical image analysis is to measure the dynamic behavior of the human heart, especially the LV. Regional characterization of the heart wall motion is necessary to isolate the severity and extent of diseases such as ischemia. Magnetic resonance and other imaging technologies can now provide time-varying 3-D images of the heart with excellent spatial resolution and reasonable temporal resolutions. Deformable models are well suited for this image analysis task.

In the simplest approach, a 2-D deformable contour model is used to segment the LV boundary in each slice of an initial image volume. These contours are then used as the initial approximation of the LV boundaries in corresponding slices of the image volume at the next time instant and are then deformed to extract the new set of LV boundaries (Ueda and Mase, 1992; Ayache *et al.*, 1992; Herlin and Ayache, 1992; Singh *et al.*, 1993; Geiger *et al.*, 1995). This temporal propagation of the deformable contours dramatically decreases the time taken to segment the LV from a sequence of image volumes over a cardiac cycle. Singh *et al.* (1993) reported a time of 15 min to perform the segmentation, considerably less than the 1.5–2 h that a human expert takes for manual segmentation. McInerney and Terzopoulos (1995a) have applied the temporal propagation approach in 3-D using a 3-D dynamic deformable 'balloon' model to track the LV (Figures 8 and 9).

In a more involved approach, Amini and Duncan (1992) used bending energy and surface curvature to track and analyze LV motion. For each time instant, two sparse subsets of surface points are created by choosing geometrically significant landmark points, one for the endocardial surface and the other for the epicardial surface of the LV. Surface patches surrounding these points are then modeled as thin, flexible plates. Making the assumption that each surface patch deforms only slightly and locally within a small time interval, for each sampled point on the first surface they construct a search area on the LV surface in the image volume at the next time instant. The best matched (i.e. minimum bending energy) point within the search window on the second surface is taken to correspond to the point on the first surface. This matching process yields a set of initial motion vectors for pairs of LV surfaces derived from a 3-D image sequence. A smoothing procedure is then performed using the initial motion vectors to generate a dense motion vector field over the LV surfaces.

Cohen *et al.* (1992a) also employed a bending energy technique in 2-D and attempt to improve on this method by adding a term to the bending energy function that tends to preserve the matching of high curvature points. Goldgof *et al.* (Goldgof *et al.*, 1988; Mishra *et al.*, 1991; Huang and Goldgof, 1993; Kambhamettu and Goldgof, 1994) have also been pursuing surface shape matching ideas primarily based on changes in Gaussian curvature and assume a conformal motion model (i.e. motion which preserves angles between curves on a surface but not distances).

An alternative approach is that of Chen *et al.* (1994), who used a hierarchical motion model of the LV constructed by combining a globally deformable superquadric with a locally deformable surface using spherical harmonic shape modeling primitives. Using this model, they estimated the LV motion from angiographic data and produced a hierarchical decomposition that characterizes the LV motion in a coarse-to-fine fashion.

Pentland and Horowitz (1991) and Nastar and Ayache (1993a, b) were also able to produce a coarse-to-fine characterization of the LV motion. They used dynamic deformable models to track and recover the LV motion and make use of modal analysis, a well-known mechanical engineering technique, to parameterize their models. This parameterization is obtained from the eigenvectors of a finite element formulation of the models. These eigenvectors are often referred to as the 'free vibration' modes and variable detail of LV motion representation results from varying the number of modes used.

The heart is a relatively smooth organ and consequently there are few reliable landmark points. The heart also undergoes complex non-rigid motion that includes a twisting (tangential) component as well as the normal component of motion. The motion recovery methods described above

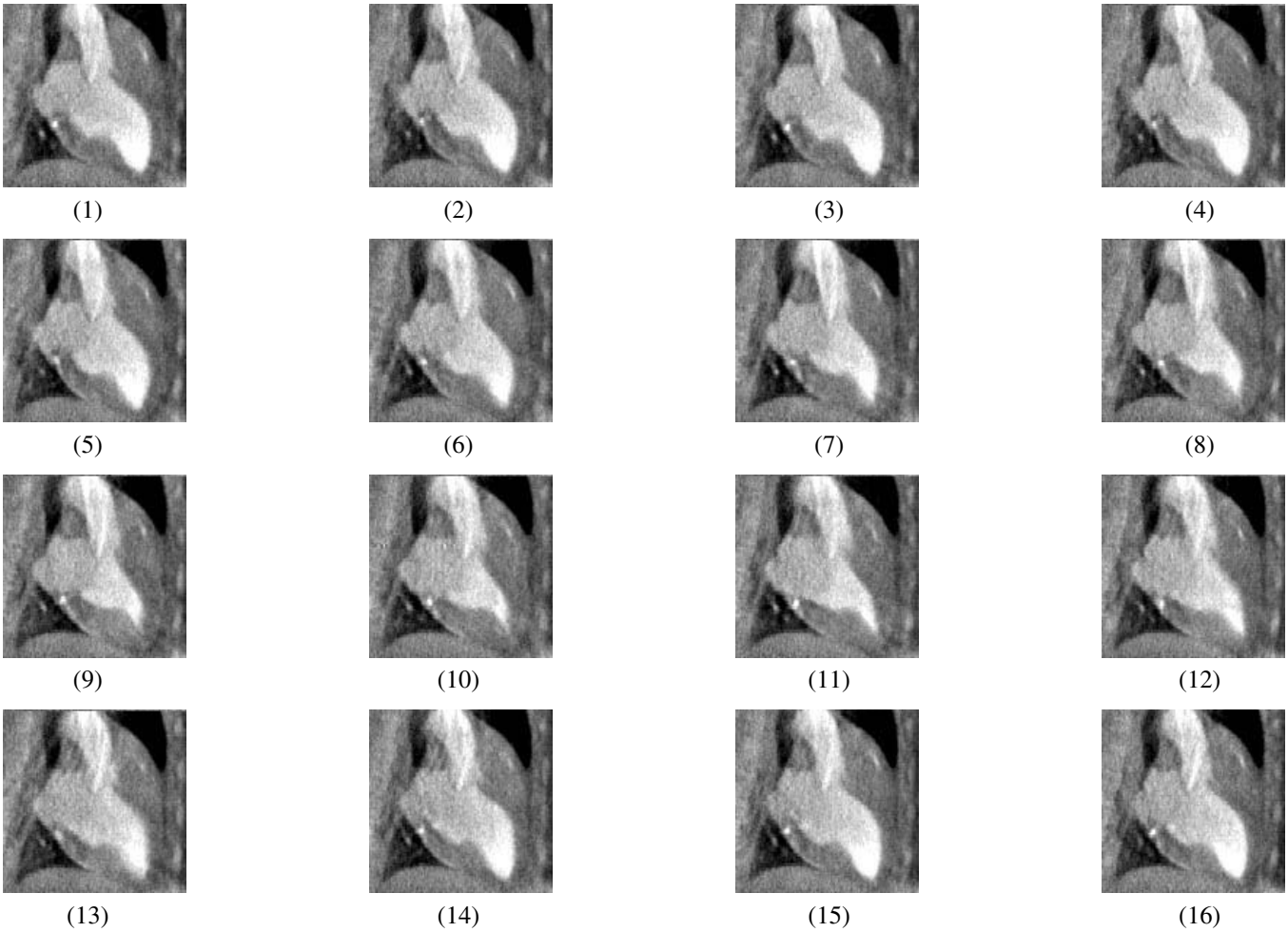


Figure 8. Sagittal slice of successive CT volumes over one cardiac cycle (1–16) showing motion of canine LV (McInerney and Terzopoulos, 1995a).

are, in general, not able to capture this tangential motion without additional information. Recently, magnetic resonance techniques, based on magnetic tagging (Axel and Dougherty, 1989) have been developed to track material points on the myocardium in a non-invasive way. The temporal correspondence of material points that these techniques provide allow for quantitative measurement of tissue motion and deformation including the twisting component of the LV motion. Several researchers have applied deformable models to image sequences of MR tagged data (Young *et al.*, 1993, 1995; Ducan *et al.*, 1994; Kumar and Goldgof, 1994; Amini *et al.*, 1995; Kraitchman *et al.*, 1995; Park *et al.*, 1996). For example, Amini *et al.* (1995) and Kumar and Goldgof (1994) used a 2-D deformable grid to localize and track SPAMM (spatial modulation of magnetization) tag points on the LV tissue. Park *et al.* (1995, 1996) fitted a volumetric physics-based deformable model to MRI-SPAMM data of the LV. The parameters of the model are functions which can capture regional shape variations of the LV such as bending, twisting and contraction. Based on this model, the authors quantitatively compared normal hearts and hearts with hypertrophic cardiomyopathy.

Another problem with most of the methods described above is that they model the endocardial and epicardial surfaces of the LV separately. In reality the heart is a thick-walled structure. Duncan *et al.* (1994) and Park *et al.* (1995, 1996) developed models which consider the volumetric nature of the heart wall. These models use the shape properties of the endocardial and epicardial surfaces and incorporate mid-wall displacement information of tagged MR images. By constructing 3-D finite element models of the LV with nodes in the mid-wall region as well as nodes on the endocardial and epicardial surfaces, more accurate measurements of the LV motion can be obtained. Young and Axel (1992, 1995) and Creswell (1992) have also

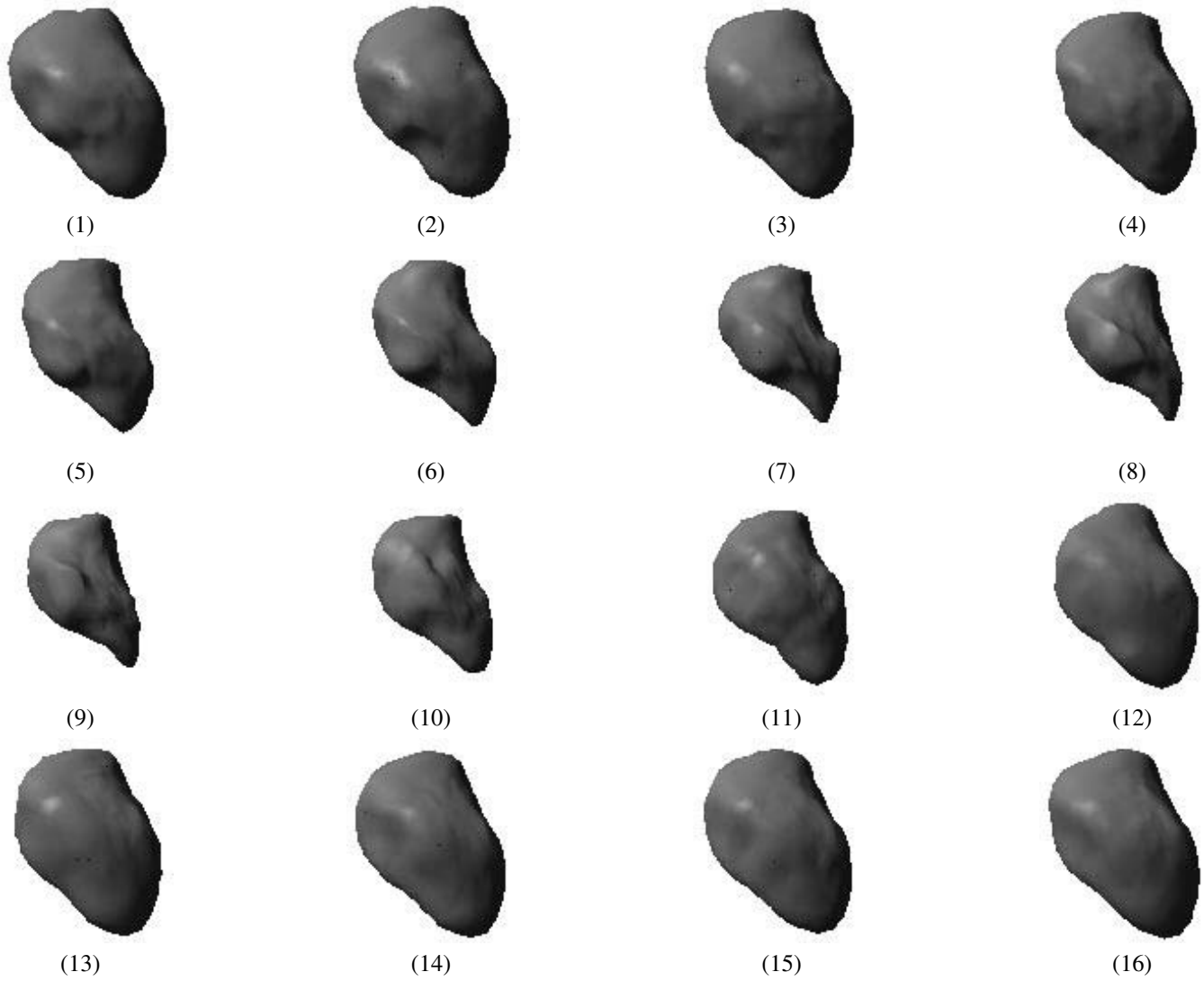


Figure 9. Tracking of the LV motion during one cardiac cycle (1–16) using deformable balloon model (McInerney and Terzopoulos, 1995a).

constructed 3-D finite element models from the boundary representations of the endocardial and epicardial surfaces.

4. DISCUSSION

In the previous sections we have surveyed the considerable and rapidly expanding body of work on deformable models in medical image analysis. The survey has revealed several issues that are relevant to the continued development of the deformable model approach. This section summarizes the key issues and indicates some promising research directions.

- Automation versus control
  Interactive (semiautomatic) algorithms and fully automatic algorithms represent two alternative approaches to computerized medical image analysis. Certainly automatic interpretation of medical images is a desirable, albeit very difficult, long-term goal, since it can potentially increase the speed, accuracy, consistency and reproducibility of the analysis. However, the interactive or semiautomatic methodology is likely to remain dominant in practice for some time to come, especially in applications where erroneous interpretations are unacceptable. Consequently, the most immediately successful deformable-model-based techniques are likely be those that drastically decrease the labor-intensiveness of medical image processing tasks through partial automation, while still allowing for interactive guidance or editing by the medical expert. Although fully automatic

techniques based on deformable models are unlikely to reach their full potential for some time to come, they can be of immediate value in specific application domains where interactive techniques are either impractical (e.g. 3-D reconstruction of complex vascular structures) or for non-critical tasks (e.g. segmentation of healthy tissue surrounding a pathology for enhanced visualization).

- Generality versus specificity
  Ideally a deformable model should be capable of representing a broad range of shapes and be useful in a wide array of medical applications. Generality is the basis of deformable model formulations with local shape parameters such as snakes. Alternatively, highly specific, 'hand-crafted' or constrained deformable models appear to be useful in applications such as tracking the non-rigid motion of the heart (section 3.5), automatically matching and labeling structures in the brain from 3-D MR images (section 3.4), or segmenting very noisy images such as echocardiograms. Certainly attempts to automate completely the processing of medical images would require a high degree of application and model specificity. A promising direction for future study appears to be techniques for learning 'tailored' models from simple general purpose models. The work of Cootes *et al.* (1994) may be viewed as an example of such a strategy.
- Compactness versus geometric coverage versus topological flexibility
  A geometric model of shape may be evaluated based on the parsimony of its formulation, its representational power and its topological flexibility. Generally, parameterized models offer the greatest parsimony, free-form (spline) models feature the broadest coverage, and implicit models have the greatest topological flexibility. Deformable models have been developed based on each of these geometric classes. Increasingly, researchers are turning to the development of hybrid deformable models that combine complementary features. For objects with a simple, fixed topology and without significant protrusions, parameterized models coupled with local (spline) and/or global deformations schemes appear to provide a good compactness–descriptiveness tradeoff (Terzopoulos and Metaxas, 1991; Pentland and Horowitz, 1991; Vemuri and Radisavljevic, 1994; Chen *et al.*, 1994). On the other hand, the segmentation and modeling of complex, multipart objects such as arterial or bronchial 'tree' structures, or topologically complex structures such as vertebrae, is a difficult task with these types of models. Polygon-based or particle-based deformable modeling schemes seem promising in segmenting and reconstructing such structures. Polygon-based models may be made compacted by removing and 'retiling' (Turk, 1992; Gourdon, 1995) polygons in regions of low shape variation, or by replacing a region of polygons with a single, high-order finite element or spline patch. A possible research direction is to develop alternative models that blend or combine descriptive primitive elements, such as flexible cylinders, into a global structure.
- Curve versus surface versus solid models
  The earliest deformable models were curves and surfaces. Anatomic structures in the human body, however, are either solid or thick-walled. To support the expanding role of medical images into tasks such as surgical planning and simulation, and the functional modeling of structures such as bones, muscles, skin or arterial blood flow, may require volumetric or solid deformable models rather than surface models. For example, the planning of facial reconstructive surgery requires the extraction and reconstruction of the skin, muscles and bones from 3-D images using accurate solid models. It also requires the ability to simulate the movement and interactions of these structures in response to forces, the ability to move, cut and fuse pieces of the model in a realistic fashion, and the ability to stimulate the simulated muscles of the model to predict the effect of the surgery. Several researchers have begun to explore the use of volumetric or solid deformable models of the human face and head for computer graphics applications (Essa *et al.*, 1993; Lee *et al.*, 1995) and for medical applications, particularly reconstructive surgery (Waters, 1992; Pieper *et al.*, 1992; Geiger, 1992; Delingette *et al.*, 1994) and there is much room for further research. Researchers have also begun to use volumetric deformable models to track and analyze LV motion more accurately (Young and Axel, 1992; Creswell *et al.*, 1992; Duncan *et al.*, 1994; Park *et al.*, 1996).
- Accuracy and quantitative power
  Ideally it should be possible to measure and control the accuracy of a deformable model. The most common accuracy control mechanisms are the global or local subdivision of model basis functions (Miller *et al.*, 1991), or the repositioning of model points to increase their density in regions of the data exhibiting rapid shape variations (Vasilescu and Terzopoulos, 1992). Other mechanisms that warrant further research are the local control and adaptation of model continuity, parameter evolution (including the rate and scheduling of the evolution), and the automation of all accuracy control mechanisms. The parametric formulation of a deformable model should not only yield an accurate description of the object, but it should also provide quantitative information about the object in an intuitive, convenient form. That is,

the model parameters should be useful for operations such as measuring, matching, modification, rendering, and higher-level analysis or geometric reasoning. This 'parameter descriptiveness' criterion may be achieved in a postprocessing step by adapting or optimizing the parameterization to match the data more efficiently or more descriptively. However, it is preferable to incorporate the descriptive parameterization directly into the model formulation. An example of this strategy is the deformable model of Park *et al.* (1995, 1996).

- Robustness
  Ideally, a deformable model should be insensitive to initial conditions and noisy data. Deformable models are able to exploit multiple image attributes and high-level or global information to increase the robustness of shape recovery. For example, many snakes models now incorporate region-based image features as well as the traditional edge-based features (section 3.1). Strategies worthy of further research include the incorporation of shape constraints into the deformable model that are derived from low-level image-processing operations such as thinning, medial axis transforms or mathematical morphology. A classical approach to improve the robustness of model fitting is the use of multiscale image preprocessing techniques (Kass *et al.*, 1988; Terzopoulos *et al.*, 1988), perhaps coupled with a multiresolution deformable model (Bajcsy and Kovacic, 1989). A multiresolution technique that merits further research in the context of deformable models is the use of wavelet bases (Strang and Nguyen, 1996) for deformations (Vemuri *et al.*, 1993; Vemuri and Radisavljevic, 1994). A deformable model should be able to easily incorporate added constraints and any other *a priori* anatomic knowledge of object shape and motion. Section 3.3 reviewed several of the most promising techniques to incorporate *a priori* knowledge. For example, for LV motion tracking, a promising research direction is the incorporation of biomechanical properties of the heart and the inclusion of the temporal periodic characteristics of the heart motion. Future directions include modeling schemes that incorporate reasoning and recognition mechanisms using techniques from artificial intelligence such as rule-based systems or neural networks.

5. CONCLUSION

The increasingly important role of medical imaging in the diagnosis and treatment of disease has opened an array of challenging problems centered on the computation of accurate geometric models of anatomic structures from medical images. Deformable models offer an attractive approach to tackling such problems, because these models are able to represent the complex shapes and broad shape variability of anatomical structures. Deformable models overcome many of the limitations of traditional low-level image-processing techniques, by providing compact and analytical representations of object shape, by incorporating anatomic knowledge, and by providing interactive capabilities. The continued development and refinement of these models should remain an important area of research into the foreseeable future.

ACKNOWLEDGEMENTS

We would like to thank Stephanie Sandor and Richard Leahy of the USC Signal and Image Processing Institute for the deformable brain atlas figure, as well as the following individuals for providing citation information that improved the completeness of the bibliography: Amir Amini, Nicholas Ayache, Ingrid Carlbom, Chang Wen Chen, James Duncan, Dmitry Goldgof, Thomas Huang, Stephane Lavallee, Francois Leitner, Gerard Medioni, Dimitri Metaxas, Alex Pentland, Stan Sclaroff, Ajit Singh, Richard Szeliski, Baba Vemuri, Alistair Young and Alan Yuille. T.M. is grateful for the financial support of an NSERC postgraduate scholarship. D.T. is a fellow of the Canadian Institute for Advanced Research. This work was made possible by the financial support of the Information Technologies Research Center of Ontario.

REFERENCES

Amini, A. A. and Duncan, J. S. (1992). Bending and stretching models for LV wall motion analysis from curves and surfaces. *Image and Vision Computing*, 10(6), 418–430.

Amini, A. A., Weymouth, T. E. and Jain, R. C. (1990). Using dynamic programming for solving variational problems in vision. *IEEE Trans. Pattern Anal. Machine Intelligence*, 12(9), 855–867.

Amini, A. A., Curwen, R. W., Klein, A. K., Egglin, T. K., Pollak, J., Lee, F. and Gore, J. C. (1995). Physics based snakes, Kalman snakes, and snake grids for feature localization and tracking in medical images. In (Bizais *et al.*, 1995), pp. 363–364.

Axel, L. and Dougherty, L. (1989). Heart wall motion: Improved method of spatial modulation of magnetization for MR imaging. *Radiology*, 172, 349–350.

Ayache, N. (1995a). Medical computer vision, virtual reality and robotics. *Image and Vision Computing*, 13(4), 295–313.

Ayache, N. (ed.) (1995b). *Proc. First International Conf. on Computer Vision, Virtual Reality and Robotics in Medicine (CVRMed'95), Nice, France, April, 1995*. Lectures Notes in Computer Science, Vol. 905. Berlin, Germany: Springer–Verlag.

Ayache, N., Cohen, I. and Herlin, I. L. (1992). Medical image tracking. Ch. 17 Blake, A. and Yuille, A. (eds), *Active Vision*. Cambridge, MA: MIT Press.

Bajcsy, R. and Kovacic, S. (1989). Multiresolution elastic matching. *Comput. Vision, Graphics Image Process.*, 46, 1–21.

Ballard, D. and Brown, C. (1982). *Computer Vision*. Englewood Cliffs, NJ: Prentice–Hall.

Bardinet, E., Cohen, L. D. and Ayache, N. (1995). Superquadrics and free-form deformations: A global model to fit and track 3D medical data. In (Ayache, 1995b), pp. 319–326.

Bardinet, E., Cohen, L. D. and Ayache, N. (1996a). *Analyzing the deformation of the left ventricle of the heart with a parametric deformable model*. Research report 2797. INRIA, Sophia-Antipolis, France.

Bardinet, E., Cohen, L. D. and Ayache, N. (1996b). A parametric deformable model to fit unstructured 3D data. *Computer Vision and Image Understanding*. In press. Also research report 2617, INRIA, Sophia-Antipolis, France.

Berger, M. O. (1990). Snake growing. In Faugeras, O. (ed.), *Computer Vision – Proc. First European Conf. on Computer Vision (ECCV'90), Antibes, France, April, 1990*, pp. 570–572, Lectures Notes in Computer Science. Springer–Verlag.

Bizais, Y., Barillot, C. and Paola, R. Di (eds) (1995). *Information Processing in Medical Imaging: Proc. 14th Int. Conf. (IPMI'95), Ile de Berder, France, June, 1995*. Computational Imaging and Vision, Vol. 3. Dordrecht, The Netherlands: Kluwer Academic.

Bookstein, F. L. (1989). Principal warps: Thin-plate splines and the decomposition of deformations. *IEEE Trans. Pattern Anal. Machine Intelligence*, 11(6), 567–585.

Bookstein, F. L. (1991). Thin-plate splines and the atlas problem for biomedical images. In Barret, H.H. and Gmitro, A.F. (eds), *Information Processing in Medical Imaging: Proc. 12th Int. Conf. (IPMI'91), Wye, UK, July, 1991*, pp. 326–342, Lectures Notes in Computer Science. Springer–Verlag.

Bozma, I. and Duncan, J. S. (1992). A modular system for image analysis using a game theoretic framework. *Image Vision Comput.*, 10(6), 431–443.

Broit, C. (1981). *Optimal Registration of Deformed Images*. Ph.D. thesis, Computer and Information Science Dept., University of Pennsylvania, Philadelphia, PA.

Carlbom, I., Terzopoulos, D. and Harris, K. (1994). Computer-assisted registration, segmentation, and 3D reconstruction from images of neuronal tissue sections. *IEEE Trans. Med. Imag.*, 13(2), 351–362.

Caselles, V., Catte, F., Coll, T. and Dibos, F. (1993). A geometric model for active contours. *Numerische Mathematik*, 66.

Caselles, V., Kimmel, R. and Sapiro, G. (1995). Geodesic active contours. In *Proc. Fifth International Conf. on Computer Vision (ICCV'95), Cambridge, MA, June, 1995*, pp. 694–699, Los Alamitos, CA: IEEE Computer Society Press.

Chakraborty, A. and Duncan, J. S. (1995). Integration of boundary finding and region-based segmentation using game theory. In (Bizais *et al.*, 1995), pp. 189–200.

Chakraborty, A., Staib, L. H. and Duncan, J. S. (1994). Deformable boundary finding influenced by region homogeneity. In *Proc. Conf. on Computer Vision and Pattern Recognition (CVPR'94), Seattle, WA, June, 1994*, Los Alamitos, CA, pp. 624–627. IEEE Computer Society Press.

Chang, L. W., Chen, H. W. and Ho, J. R. (1991). Reconstruction of 3D medical images: A nonlinear interpolation technique for reconstruction of 3D medical images. *Comput. Vision, Graphics Image Process.*, 53(4), 382–391.

Chen, C. W., Huang, T. S. and Arrott, M. (1994). Modeling, analysis and visualization of left ventricle shape and motion by hierarchical decomposition. *IEEE Trans. Pattern Anal. Machine Intelligence*, 16(April), 342–356.

Christensen, G., Rabbitt, R. D., Miller, M. I., Joshi, S. C., Grenander, U., Coogan, T. A. and van Essen, D. C. (1995). Topological properties of smooth anatomic maps. In (Bizais *et al.*, 1995), pp. 101–112.

Cohen, I., Ayache, N. and Sulger, P. (1992a). Tracking points on deformable objects using curvature information. In Sandini, G. (ed.), *Computer Vision – Proc. Second European Conf. on Computer Vision (ECCV'92), Santa Margherita Ligure, Italy, May, 1992*, pp. 458–466, Lectures Notes in Computer Science. Springer–Verlag.

Cohen, I., Cohen, L. D. and Ayache, N. (1992b). Using deformable surfaces to segment 3D images and infer differential structures. *CVGIP: Image Understanding*, 56(2), 242–263.

Cohen, L. D. (1991). On active contour models and balloons. *CVGIP: Image Understanding*, 53(2), 211–218.

Cohen, L. D. and Cohen, I. (1993). Finite element methods for active contour models and balloons for 2D and 3D images. *IEEE Trans. Pattern Anal. Machine Intelligence*, 15(11), 1131–1147.

Cootes, T., Hill, A., Taylor, C. and Haslam, J. (1994). The use of active shape models for locating structures in medical images. *Image Vision Comput.*, 12(6), 355–366.

Creswell, L. L., Wyers, S. G., Pirolo, J. S., Perman, W. H., Vannier, M. W. and Pasque, M. K. (1992). Mathematical modelling of the heart using magnetic resonance imaging. *IEEE Trans. Med. Imag.*, 11(4), 581–589.

Davatzikos, C. and Bryan, R. N. (1995). Using a deformable surface model to obtain a mathematical representation of the cortex. In *International Symp. on Computer Vision, Coral Gables, FL, November, 1995*, pp. 212–217, Los Alamitos, CA: IEEE Computer Society Press.

Davatzikos, C. A. and Prince, J. L. (1995). An active contour model for mapping the cortex. *IEEE Trans. Med. Imag.*, 14(1), 65–80.

Davatzikos, C. A., Prince, J. L. and Bryan, R. N. (1996). Image registration based on boundary mapping. *IEEE Trans. Med. Imag.*, 15(1), 112–115.

Declerck, J., Subsol, G., Thirion, J. P. and Ayache, N. (1995). Automatic retrieval of anatomic structures in 3D medical images. In (Ayache, 1995b), pp. 153–162.

Delibasis, K. and Undrill, P. E. (1994). Anatomical object recognition using deformable geometric models. *Image Vision Comput.*, 12(7), 423–433.

Delingette, H., Hebert, M. and Ikeuchi, K. (1992). Shape representation and image segmentation using deformable surfaces. *Image Vision Comput.*, 10(3), 132–144.

Delingette, H., Subsol, G., Cotin, S. and Pignon, J. (1994). Virtual reality and craniofacial surgery simulation. In (Robb, 1994), pp. 607–618.

Duncan, J. *et al.* (1994). Towards reliable, noninvasive measurement of myocardial function from 4D images. In *Medical Imaging 1994: Physiology and Function from Multidimensional Medical*

Images, SPIE Proc., Vol. 2168, pp. 149–161, Bellingham, WA: SPIE.

Essa, I., Sclaroff, S. and Pentland, A. P. (1993). Physically-based modeling for graphics and vision. In Martin, R. (ed.), *Directions in Geometric Computing*. Information Geometers, U.K.

Evans, A. C., Dai, W., Collins, L., Neelin, P. and Marrett, S. (1991). Warping of a computerized 3D atlas to match brain image volumes for quantitative neuroanatomical and functional analysis. In *Medical Imaging V: Image Processing*, SPIE Proc., Vol. 1445, pp. 236–246, Bellingham, WA: SPIE.

Farin, G. (1993). *Curves and Surfaces for CAGD*. New York, NY: Academic Press.

Feldmar, J. and Ayache, N. (1994). Locally affine registration of free-form surfaces. In *Proc. Conf. on Computer Vision and Pattern Recognition (CVPR'94), Seattle, WA, June, 1994*, pp. 496–501, Los Alamitos, CA: IEEE Computer Society Press.

Fischler, M. and Elschlager, R. (1973). The representation and matching of pictorial structures. *IEEE Trans. on Computers*, 22(1), 67–92.

Gauch, J. M., Pien, H. H. and Shah, J. (1994). Hybrid boundary-based and region-based deformable models for biomedical image segmentation. In *Mathematical Methods in Medical Imaging III*, SPIE Proc., Vol. 2299, pp. 72–83, San Diego, CA: SPIE.

Gee, J., Reivich, M. and Bajcsy, R. (1993). Elastically deforming 3D atlas to match anatomical brain images. *Journal of Computer Assisted Tomography*, 17(2), 225–236.

Geiger, B. (1992). Three dimensional simulation of delivery for cephalopelvic disproportion. In *First International Workshop on Mechatronics in Medicine and Surgery, Costa del Sol, Spain, October, 1992*, pp. 146–152.

Geiger, D., Gupta, A., Costa, L. A. and Vlontzos, J. (1995). Dynamic programming for detecting, tracking and matching deformable contours. *IEEE Trans. Pattern Anal. Machine Intelligence*, 17(3), 294–302.

Goldgof, D. B., Lee, H. and Huang, T. S. (1988). Motion analysis of nonrigid surfaces. In *Proc. Conf. on Computer Vision and Pattern Recognition (CVPR'88), Ann Arbor, MI, June, 1988*, pp. 375–380, Los Alamitos, CA: IEEE Computer Society Press.

Gourdon, A. (1995). Simplification of irregular surface meshes in 3D medical images. In (Ayache, 1995b), pp. 413–419.

Grzeszczuk, R. P. and Levin, D. N. (1994). Brownian strings: Segmenting images with stochastically deformable contours. In (Robb, 1994), pp. 72–89.

Gueziec, A. and Ayache, N. (1994). Smoothing and matching of 3D space curves. *Int. J. Comput. Vision*, 12(1), 79–104.

Gupta, A., O'Donnell, T. and Singh, A. (1994). Segmentation and tracking of cine cardiac MR and CT images using a 3-D deformable model. In *Proc. IEEE Conf. on Computers in Cardiology, September, 1994*.

Gwydir, S. H., Buettner, H. M. and Dunn, S. M. (1994). Non-rigid motion analysis and feature labelling of the growth cone. In *IEEE Workshop on Biomedical Image Analysis, Seattle, WA, June, 1994*, pp. 80–87, Los Alamitos, CA: IEEE Computer Society Press.

Hamadeh, A., Lavallee, S., Szeliski, R., Cinquin, P. and Peria, O. (1995). Anatomy-based registration for computer-integrated surgery. In (Ayache, 1995b), pp. 212–218.

Herlin, I. L. and Ayache, N. (1992). Features extraction and analysis methods for sequences of ultrasound images. *Image Vision Comput.*, 10(10), 673–682.

Herlin, I. L., Nguyen, C. and Graffigne, C. (1992). A deformable region model using stochastic processes applied to echocardiographic images. In *Proc. Conf. on Computer Vision and Pattern Recognition (CVPR'92), Urbana, IL, June, 1992*, pp. 534–539, Los Alamitos, CA: IEEE Computer Society Press.

Hill, A., Thornham, A. and Taylor, C. J. (1993). Model-based interpretation of 3D medical images. In *Proc. 4th British Machine Vision Conf. (BMVC'93), Surrey, UK, September, 1993*, pp. 339–348, BMVA Press.

Huang, W. C. and Goldgof, D. B. (1993). Adaptive-size meshes for rigid and nonrigid shape analysis and synthesis. *IEEE Trans. Pattern Anal. Machine Intelligence*, 15(3).

Kambhamettu, C. and Goldgof, D. B. (1994). Point correspondence recovery in nonrigid motion. *CVGIP: Image Understanding*, 60(1), 26–43.

Kass, M., Witkin, A. and Terzopoulos, D. (1988). Snakes: Active contour models. *Int. J. Comput. Vision*, 1(4), 321–331.

Kraitchman, D. L., Young, A. A., Chang, C. N. and Axel, L. (1995). Semi-automatic tracking of myocardial motion in MR tagged images. *IEEE Trans. Med. Imag.*, 14(3), 422–432.

Kumar, S. and Goldgof, D. (1994). Automatic tracking of SPAMM grid and the estimation of deformation parameters from cardiac MR images. *IEEE Trans. Med. Imag.*, 13(1), 122–132.

Lavallée, S. and Szeliski, R. (1995). Recovering the position and orientation of free-form objects from image contours using 3D distance maps. *IEEE Trans. Pattern Anal. Machine Intelligence*, 17(4), 378–390.

Lee, Y., Terzopoulos, D. and Waters, K. (1995). Realistic modeling for facial animation. In *Proc. SIGGRAPH'95, Los Angeles, CA, August, 1995, in Computer Graphics Proc., Annual Conf. Series 1995*, pp. 55–62, New York, NY: ACM SIGGRAPH.

Leitner, F. and Cinquin, P. (1991). Complex topology 3D objects segmentation. In *Model-Based Vision Development and Tools*, SPIE Proc., Vol. 1609, pp. 16–26, Bellingham, WA: SPIE.

Leitner, F. and Cinquin, P. (1993). From splines and snakes to Snakes Splines. In Laugier, C. (ed.), *Geometric Reasoning: From Perception to Action*, Lectures Notes in Computer Science, Vol. 708, pp. 264–281, Springer–Verlag.

Lengyel, J., Greenberg, D. P. and Popp, R. (1995). Time-dependent three-dimensional intravascular ultrasound. In *Proc. SIGGRAPH'95, Los Angeles, CA, August, 1995, in Computer Graphics Proc., Annual Conf. Series 1995*, pp. 457–464, New York, NY: ACM SIGGRAPH.

Leymarie, F. and Levine, M. (1993). Tracking deformable objects in the plane using an active contour model. *IEEE Trans. Pattern Anal. Machine Intelligence*, 15(6), 635–646.

Lin, W. C. and Chen, S. Y. (1989). A new surface interpolation technique for reconstructing 3D objects from serial cross-

sections. *Comput. Vision, Graphics Image Process.*, 48(Oct.), 124–143.

Lipson, P., Yuille, A. L., O'Keefe, D., Cavanaugh, J., Taaffe, J. and Rosenthal, D. (1990). Deformable templates for feature extraction from medical images. In Faugeras, O. (ed.), *Computer Vision – Proc. First European Conf. on Computer Vision (ECCV'90), Antibes, France, April, 1990*, pp. 477–484, Lectures Notes in Computer Science. Springer–Verlag.

Lobregt, S. and Viergever, M. A. (1995). A discrete dynamic contour model. *IEEE Trans. Med. Imag.*, 14(1), 12–24.

Malladi, R., Sethian, J. and Vemuri, B. C. (1995). Shape modeling with front propagation: A level set approach. *IEEE Trans. Pattern Anal. Machine Intelligence*, 17(2), 158–175.

Mangin, J. F., Tupin, F., Frouin, V., Bloch, I., Rougetet, R., Regis, J. and Lopez-Krahe, J. (1995). Deformable topological models for segmentation of 3D medical images. In (Bizais *et al.*, 1995), pp. 153–164.

McDonald, D., Avis, D. and Evans, A. (1994). Multiple surface identification and matching in magnetic resonance images. In (Robb, 1994), pp. 160–169.

McInerney, T. and Terzopoulos, D. (1995a). A dynamic finite element surface model for segmentation and tracking in multidimensional medical images with application to cardiac 4D image analysis. *Computerized Medical Imaging and Graphics*, 19(1), 69–83.

McInerney, T. and Terzopoulos, D. (1995b). Topologically adaptable snakes. In *Proc. Fifth International Conf. on Computer Vision (ICCV'95), Cambridge, MA, June, 1995*, pp. 840–845, Los Alamitos, CA: IEEE Computer Society Press.

Metaxas, D. and Terzopoulos, D. (1993). Shape and nonrigid motion estimation through physics-based synthesis. *IEEE Trans. Pattern Anal. Machine Intelligence*, 15(6), 580–591.

Miller, J. V., Breen, D. E., Lorensen, W. E., O'Bara, R. M. and Wozny, M. J. (1991). Geometrically deformed models: A method for extracting closed geometric models from volume data. In *Computer Graphics (Proc. SIGGRAPH'91 Conf., Las Vegas, NV, July, 1991)*, Vol. 25(4), pp. 217–226.

Mishra, S. K., Goldgof, D. B. and Huang, T. S. (1991). Non-rigid motion analysis and epicardial deformation estimation from angiography data. In *Proc. Conf. on Computer Vision and Pattern Recognition (CVPR'91), Maui, HI, June, 1991*, pp. 331–336, Los Alamitos, CA: IEEE Computer Society Press.

Moshfeghi, M. (1991). Elastic matching of multimodality medical images. *CVGIP: Graphical Models and Image Processing*, 53, 271–282.

Moshfeghi, M., Ranganath, S. and Nawyn, K. (1994). Three-dimensional elastic matching of volumes. *IEEE Trans. on Image Processing*, 3, 128–138.

Nastar, C. and Ayache, N. (1993a). Fast segmentation, tracking, and analysis of deformable objects. In *Proc. Fourth International Conf. on Computer Vision (ICCV'93), Berlin, Germany, May, 1993*, pp. 275–279, Los Alamitos, CA: IEEE Computer Society Press.

Nastar, C. and Ayache, N. (1993b). Non-rigid motion analysis in medical images: A physically based approach. In Colchester, A.C.F. and Hawkes, D.J. (eds), *Information Processing in Medical Imaging: Proc. 13th Int. Conf. (IPMI'93), Flagstaff, AZ, June, 1993*, pp. 17–32, Lectures Notes in Computer Science. Springer–Verlag.

Park, J., Metaxas, D. and Axel, L. (1995). Volumetric deformable models with parameter functions: A new approach to the 3D motion analysis of the LV from MRI–SPAMM. In *Proc. Fifth International Conf. on Computer Vision (ICCV'95), Cambridge, MA, June, 1995*, pp. 700–705, Los Alamitos, CA: IEEE Computer Society Press.

Park, J., Metaxas, D. and Axel, L. (1996). Analysis of left ventricular wall motion based on volumetric deformable models and MRI-SPAMM. *Medical Image Analysis*, 1(1), 53–72.

Pentland, A. and Horowitz, B. (1991). Recovery of nonrigid motion and structure. *IEEE Trans. Pattern Anal. Machine Intelligence*, 13(7), 730–742.

Pentland, A. and Sclaroff, S. (1991). Closed-form solutions for physically based shape modelling and recognition. *IEEE Trans. Pattern Anal. Machine Intelligence*, 13(7), 715–729.

Pieper, S., Rosen, J. and Zeltzer, D. (1992). Interactive graphics for plastic surgery: A task-level analysis and implementation. In *Proc. ACM 1992 Symposium on Interactive 3D Graphics*, pp. 127–134.

Poon, C. S., Braun, M., Fahrig, R., Ginige, A. and Dorrell, A. (1994). Segmentation of medical images using an active contour model incorporating region-based images features. In (Robb, 1994), pp. 90–97.

Press, W. H., Teukolsky, S. A., Vetterling, W. T. and Flannery, B. P. (1992). *Numerical Recipes in C*. Cambridge University Press.

Robb, R. A. (ed.) (1994). *Proc. Third Conf. on Visualization in Biomedical Computing (VBC'94), Rochester, MN, October, 1994*. SPIE Proc., Vol. 2359, Bellingham, WA: SPIE.

Rougon, N. and Prêteux, F. (1991). Deformable markers: Mathematical morphology for active contour models control. In *Image Algebra and Morphological Image Processing II* SPIE Proc., Vol. 1568, pp. 78–89, Bellingham, WA: SPIE.

Rougon, N. and Prêteux, F. (1993). Directional adaptive deformable models for segmentation with application to 2D and 3D medical images. In *Medical Imaging 93: Image Processing*, SPIE Proc., Vol. 1898, pp. 193–207, Bellingham, WA: SPIE.

Sandor, S. and Leahy, R. (1995). Towards automatic labelling of the cerebral cortex using a deformable atlas model. In (Bizais *et al.*, 1995), pp. 127–138.

Sapiro, G., Kimmel, R. and Caselles, V. (1995). Object detection and measurements in medical images via geodesic deformable contours. In *Vision Geometry IV*, SPIE Proc., Vol. 2573, pp. 366–378, Bellingham, WA: SPIE.

Singh, A., von Kurowski, L. and Chiu, M. Y. (1993). Cardiac MR image segmentation using deformable models. In *Biomedical Image Processing and Biomedical Visualization*, SPIE Proc., Vol. 1905, pp. 8–28, Bellingham, WA: SPIE.

Snell, J. W., Merickel, M. B., Ortega, J. M., Goble, J. C., Brookeman, J. R. and Kassell, N. F. (1995). Model-based boundary estimation of complex objects using hierarchical active surface templates. *Pattern Recog.*, 28(10), 1599–1609.

Staib, L. H. and Duncan, J. S. (1992a). Boundary finding with parametrically deformable models. *IEEE Trans. Pattern Anal. Machine Intelligence*, 14(11), 1061–1075.

Staib, L. H. and Duncan, J. S. (1992b). Deformable Fourier models for surface finding in 3D images. In Robb, R. A. (ed.), *Proc. Second Conf. on Visualization in Biomedical Computing (VBC'92), Chapel Hill, NC, October, 1992*, SPIE Proc., Vol. 1808, pp. 90–104, Bellingham, WA: SPIE.

Strang, G. and Nguyen, T. (1996). *Wavelets and Filter Banks*. Wellesley, MA: Wellesley-Cambridge Press.

Stytz, M., Frieder, G. and Frieder, O. (1991) Three-dimensional medical imaging: Algorithms and computer systems. *ACM Computing Surveys*, 23, 421–499.

Subsol, G., Thirion, J.Ph. and Ayache, N. (1995). A general scheme for automatically building 3D morphometric anatomical atlases: Application to a skull atlas. In *Proc. Second International Symp. on Medical Robotics and Computer Assisted Surgery (MRCAS'95), Baltimore, MD, November, 1995*, pp. 226–233.

Székely, G., Kelemen, A., Brechbuhler, Ch. and Gerig, G. (1996). Segmentation of 2-D and 3-D objects from MRI volume data using constrained elastic deformations of flexible Fourier surface models. *Medical Image Analysis*, 1(1), 19–34.

Szeliski, R. (1990). Bayesian modeling of uncertainty in low-level vision. *Int. J. Comput. Vision*, 5, 271–301.

Szeliski, R., Tonnesen, D. and Terzopoulos, D. (1993). Modeling surfaces of arbitrary topology with dynamic particles. In *Proc. Conf. on Computer Vision and Pattern Recognition (CVPR'93), New York, NY, June, 1993*, pp. 82–87, Los Alamitos, CA: IEEE Computer Society Press.

Tek, H. and Kimia, B. (1995). Shock-based reaction-diffusion bubbles for image segmentation. In (Ayache, 1995b), pp. 434–438.

Terzopoulos, D. (1986a). *On Matching Deformable Models to Images*. Tech. rept. 60. Schlumberger Palo Alto Research. Reprinted in *Topical Meeting on Machine Vision,* Technical Digest Series, Vol. 12, (Optical Society of America, Washington, DC) 1987, 160–167.

Terzopoulos, D. (1986b). Regularization of inverse visual problems involving discontinuities. *IEEE Trans. Pattern Anal. Machine Intelligence*, 8(4), 413–424.

Terzopoulos, D. and Fleischer, K. (1988). Deformable models. *The Visual Computer*, 4(6), 306–331.

Terzopoulos, D. and Metaxas, D. (1991). Dynamic 3D models with local and global deformations: Deformable superquadrics. *IEEE Trans. Pattern Anal. Machine Intelligence*, 13(7), 703–714.

Terzopoulos, D. and Szeliski, R. (1992). Tracking with Kalman snakes. In Blake, A. and Yuille, A. (eds), *Active Vision*, pp. 3–20, Cambridge, MA: MIT Press.

Terzopoulos, D., Witkin, A. and Kass, M. (1988). Constraints on deformable models: Recovering 3D shape and nonrigid motion. *Artif. Intelligence*, 36(1), 91–123.

Thirion, J. P. (1994). Extremal points: Definition and application to 3D image registration. In *Proc. Conf. on Computer Vision and Pattern Recognition (CVPR'94), Seattle, WA, June, 1994*, pp. 587–592, Los Alamitos, CA: IEEE Computer Society Press.

Turk, G. (1992). Re-tiling polygonal surfaces. In *Computer Graphics (Proc. SIGGRAPH'92 Conf., Chicago, IL, July, 1992)*, Vol. 26(2), pp. 55–64, ACM SIGGRAPH.

Ueda, N. and Mase, K. (1992). Tracking moving contours using energy-minimizing elastic contour models. In Sandini, G. (ed.), *Computer Vision – Proc. Second European Conf. on Computer Vision (ECCV'92), Santa Margherita Ligure, Italy, May, 1992*, pp. 453–457, Lectures Notes in Computer Science. Springer–Verlag.

Vasilescu, M. and Terzopoulos, D. (1992). Adaptive meshes and shells: Irregular triangulation, discontinuities and hierarchical subdivision. In *Proc. Conf. on Computer Vision and Pattern Recognition (CVPR'92), Urbana, IL, June, 1992*, pp. 829–832, Los Alamitos, CA: IEEE Computer Society Press.

Vemuri, B. C. and Radisavljevic, A. (1994). Multiresolution stochastic hybrid shape models with fractal priors. *ACM Trans. on Graphics*, 13(2), 177–207.

Vemuri, B. C., Radisavljevic, A. and Leonard, C. (1993). Multiresolution 3D stochastic shape models for image segmentation. In Colchester, A. C. F. and Hawkes, D. J. (eds), *Information Processing in Medical Imaging: Proc. 13th Int. Conf. (IPMI'93), Flagstaff, AZ, June, 1993*, pp. 62–76, Lectures Notes in Computer Science. Springer–Verlag.

Waters, K. (1992). A physical model of facial tissue and muscle articulation derived from computer tomography data. In Robb, R. A. (ed.), *Proc. Second Conf. on Visualization in Biomedical Computing (VBC'92), Chapel Hill, NC, October, 1992*, SPIE Proc., Vol. 1808, pp. 574–583, Bellingham, WA: SPIE.

Whitaker, R. (1994). Volumetric deformable models. In (Robb, 1994).

Widrow, B. (1973). The rubber mask technique, part I. *Pattern Recognition*, 5(3), 175–211.

Worring, M., Smeulders, A. W. M., Staib, L. H. and Duncan, J. S. (1993). Parameterized feasible boundaries in gradient vector fields. In Colchester, A. C. F. and Hawkes, D. J. (eds), *Information Processing in Medical Imaging: Proc. 13th Int. Conf. (IPMI'93), Flagstaff, AZ, June, 1993*, pp. 48–61, Lectures Notes in Computer Science. Springer–Verlag.

Young, A. and Axel, L. (1992). Non-rigid wall motion using MR tagging. In *Proc. Conf. on Computer Vision and Pattern Recognition (CVPR'92), Urbana, IL, June, 1992*, pp. 399–404, Los Alamitos, CA: IEEE Computer Society Press.

Young, A. A., Axel, L., Dougherty, L., Bogen, D. K. and Parenteau, C. S. (1993). Validation of tagging with MR imaging to estimate material deformation. *Radiology*, 188, 101–108.

Young, A. A., Kraitchman, D. L., Dougherty, L. and Axel, L. (1995). Tracking and finite element analysis of stripe deformation in magnetic resonance tagging. *IEEE Trans. Med. Imag.*, 14(3), 413–421.

Yuille, A. L., Hallinan, P. W. and Cohen, D. S. (1992). Feature extraction from faces using deformable templates. *Int. J. Comput. Vision*, 8, 99–111.

Zienkiewicz, O. C. and Taylor, R. L. (1989). *The Finite Element Method*. New York, NY: McGraw–Hill.